Assessment of Mechanism of Pore Formation in Directionally Solidified A356 Alloy

M. Uludağ [a], D. Dişpinar [b]

[a] Faculty of Engineering, Metallurgical and Materials Eng. Dept, Selcuk University, Konya, Turkey
[b] Faculty of Engineering, Metallurgical and Materials Eng. Dept., Istanbul University, Istanbul, Turkey
*Corresponding author. E-mail address: dr.uludagm@gmail.com

Abstract

It is well-known that the better the control of the liquid aluminium allows obtaining of better properties. One of the most important defects that is held responsible for lower properties has been the presence of porosity. Porosity has always been associated with the amount of dissolved hydrogen in the liquid. However, it was shown that hydrogen was not the major source but only a contributor the porosity. The most important defect that causes porosity is the presence of bifilms. These defects are surface entrained mainly due to turbulence and uncontrolled melt transfer. In this work, a cylindrical mould was designed (Ø30 x 300 mm) both from sand and die. Moulds were produced both from sand and die. Water cooled copper chill was placed at the bottom of the mould in order to generate a directional solidification. After the melt was prepared, prior to casting of the DC cast samples, reduced pressure test sample was taken to measure the melt quality (i.e. bifilm index). The cast parts were then sectioned into regions and longitudinal and transverse areas were investigated metallographically. Pore size, shape and distribution was measured by image analysis. The formation of porosity was evaluated by means of bifilm content, size and distribution in A356 alloy.

Keywords: Directional solidification, Porosity, Bifilm index, Grain refinement, Casting

1. Introduction

Al-7Si alloys are used in many parts of automobiles such as wheels. The properties of this alloys depend on the microstructure which is mainly affected by the solidification conditions and chemical composition [1, 2]. The microstructure is a function of rate of advancement of solid/liquid interface (i.e. cooling rate). This is controlled by the direction and amount of heat flow [3]. Therefore, typical parameters that have been investigated involves the works on heat flow and mass flow. Particularly, pore formation can be evaluated during these studies. The amount of shrinkage can be analysed by means of using a directional

solidification apparatus. Large risers, wide thickness, insulating sleeves and chills can be used to achieve such conditions [4]. The physical mechanism of columnar-to-equiaxed transition (CET) during directional solidification have been considered as the critical point during these studies [5-9].

Typically, in order to obtain finer grain structure, several grain refiners have been studied. It has been shown that the level of defects cease to decrease with increased area of grain boundary and decreased grain size [1]. For Al-Si alloys, Al-Ti-B grain refiners can be added to alter the coarse α-Al to finer dendrites without changing the morphology of eutectic Si [10].

As an alternative to Ti grain refinement, Al-3B alloy can also be used. This master alloy contains B, AlB_2 and AlB_{12}

particulates. AlB_{12} can be unstable depending on the B content of the melt; and reacts with Al to form AlB_2 which is a peritectic reaction [11, 12].

Porosity has been considered as the major defect that needs to be eliminated in cast parts. Therefore, the effect of casting conditions and alloying elements have been the focal point to investigate the pore formation in aluminium castings. Dispinar [13] has carried out an extensive study with reduced pressure test (RPT) and showed that hydrogen was not the major source of porosity. He proposed an index that could be used to quantify aluminium melt quality by measuring the sum of maximum length of pores and called it bifilm index [14]. A detailed explanation of how bifilm index is measured was given in Ref [15].

In this work, A356 alloy was used to investigate the porosity distribution in directional solidification. Grain refiners were added and the effect of melt quality over the size and distribution of porosity was evaluated.

2. Experimental Work

The composition of the alloy used in the experiments is given in Table 1. The alloy was a primary alloy obtained from a primary foundry plant in Turkey.

Table 1.
Chemical composition of A356 alloy

Si	Fe	Cu	Mn	Mg	Zn	Ti	Al
6.80	0.19	0.003	0.001	0.30	0.011	0.108	Rem.

Copper chill with a water cooling channels was used in the experiments in order to create a directional solidification was shown in Figure 1. Tap water at 20°C was used to circulate through the channels. As seen in figure, two simultaneous castings were made where the dimension was Ø30 by 300 mm

samples were produced. Castings were made into the mould cavity when the melt temperature was at 740°C.

After the castings were complete, sample collection was carried out from various heights and directions as shown in Figure 2. Five samples were horizontally cut which had 6 mm height. And each of these cylinders were sectioned into four pieces as top and bottom; and left and right, in order to investigate the porosity vertically and horizontally.
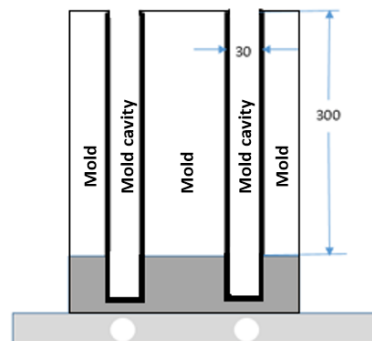

Fig. 1. Directional solidification apparatus used in the experiments

Two melts were prepared; one of them was modified with Ti grain refinement and the second melt was modified with Ti-free B grain refiner. Degassing was carried out for 20 minutes with Ar and macrostructural investigations were made for each of the melts before and after degassing. Image analysis software (Clemex) was used to measure pore size and distribution. A detailed, step-by-step explanation was given by Dispinar [15]. Reduced Pressure Test (RPT) samples were collected at 100 mbar to be solidified in a sand mould; and thereby, bifilm index measurements were made to correlate melt quality with the porosity distribution.
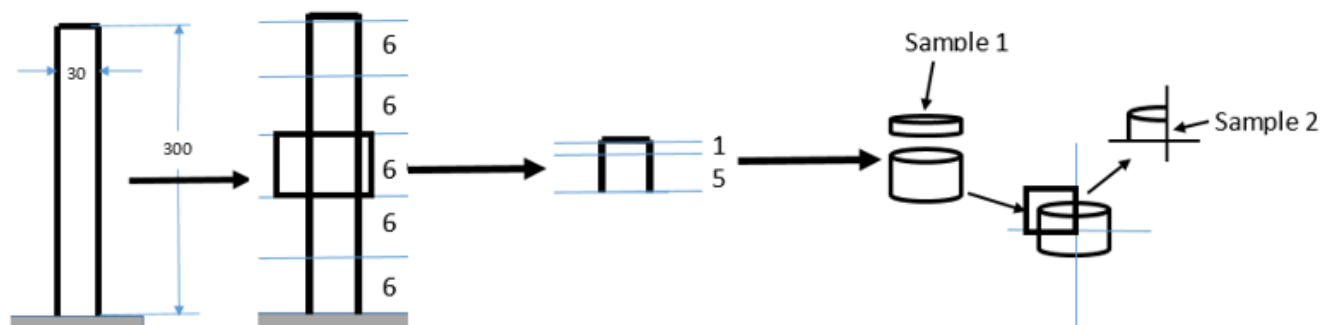

Fig. 2. Preparation of sectioned surfaces of the cast part for examining

3. Results and dıscussıon

Bifilm index measurement results of both castings before and after degassing is given in Figure 3. As can be seen, before degassing, bifilm index is around 40 mm and is has been

decreased down to 9 mm which indicated that melt quality was increased.

The macro images of the vertical sections of castings are given in Figure 4. In this figure, U1-U4 stands for the position of the sample, 1 being the top and 4 being the bottom. The clearest observation was the decrease of pore size and number from top to

the bottom (U1 towards U4). In addition, pores were decreasing even further after degassing with the decrease of bifilm index.
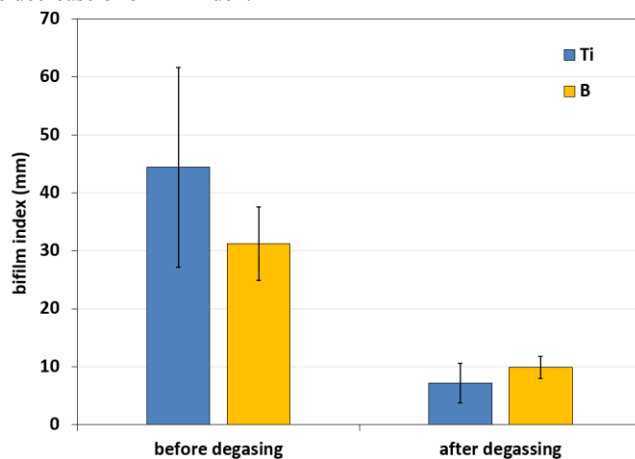

Fig. 3. Bifilm index measurements

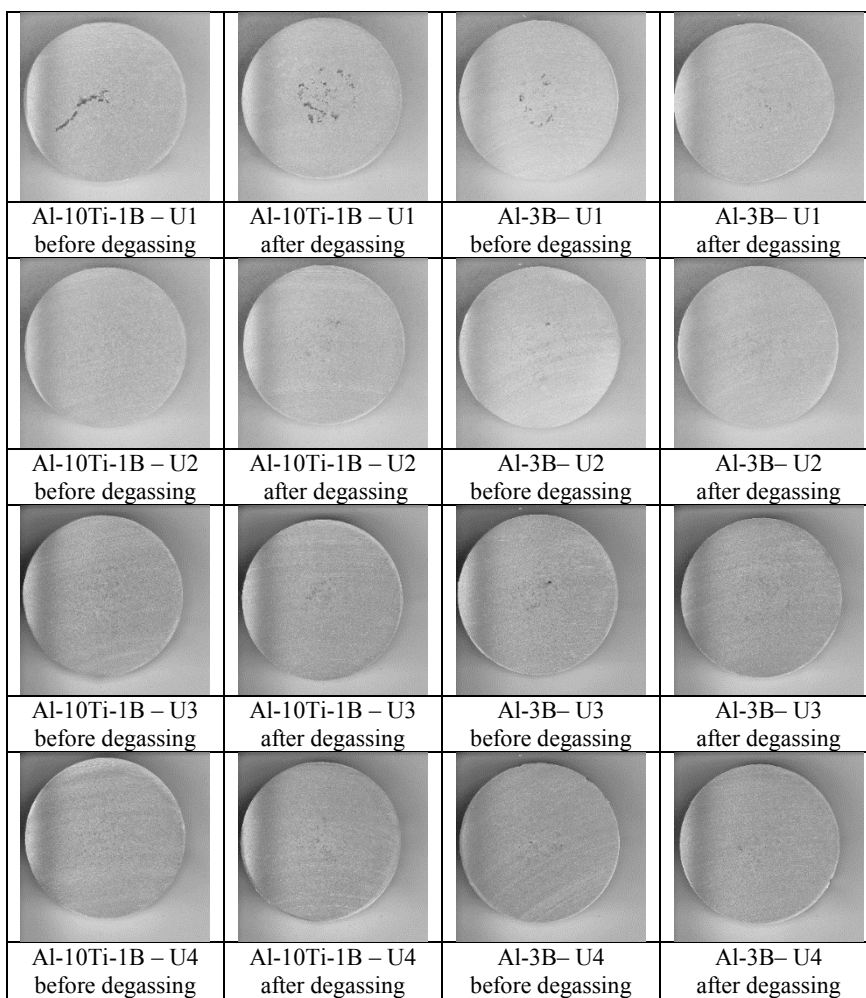| Al-10Ti-1B – U1 before degassing | Al-10Ti-1B – U1 after degassing | Al-3B– U1 before degassing | Al-3B– U1 after degassing |
Al-10Ti-1B – U2 before degassing	Al-10Ti-1B – U2 after degassing	Al-3B– U2 before degassing	Al-3B– U2 after degassing
Al-10Ti-1B – U3 before degassing	Al-10Ti-1B – U3 after degassing	Al-3B– U3 before degassing	Al-3B– U3 after degassing
Al-10Ti-1B – U4 before degassing	Al-10Ti-1B – U4 after degassing	Al-3B– U4 before degassing	Al-3B– U4 after degassing

Fig. 4. Top view (vertical) of directionally solidified samples at various heights
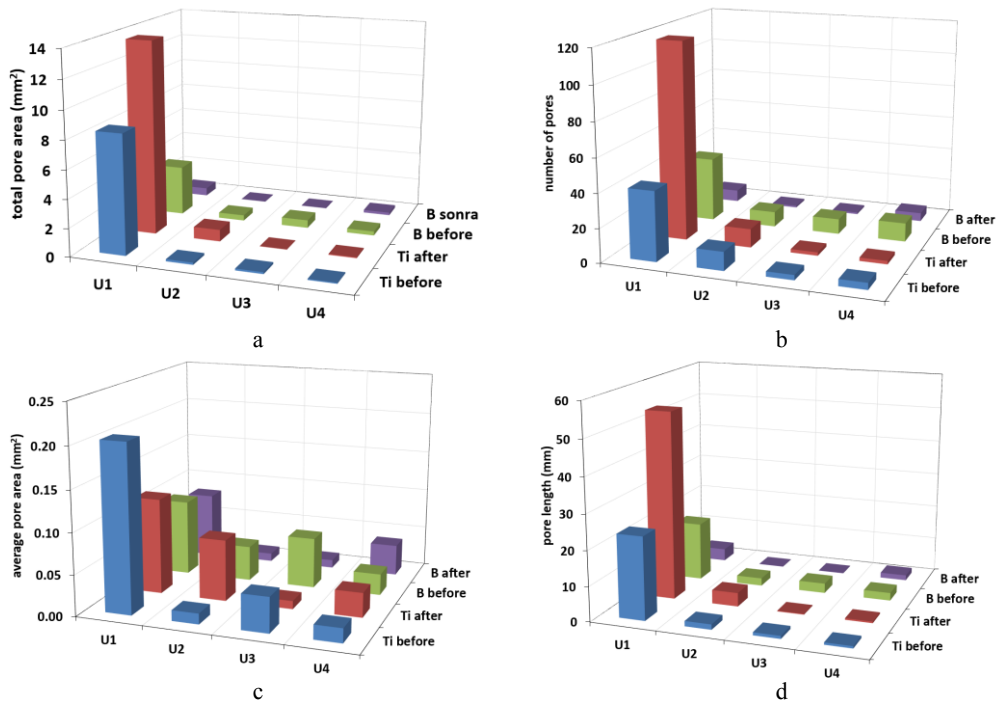
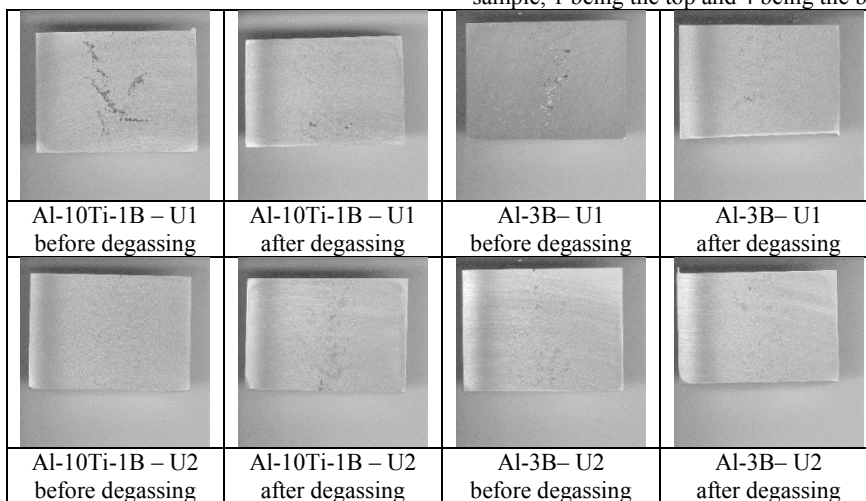Fig. 5. Porosity results of samples taken from the vertical sections.
a) total pore area, b) number of pores, c) average pore area, d) pore length (Before and after donates to "degassing") (U donates location)

All the samples were subjected to image analysis and pore size, number, area and distribution results obtained from Figure 4 can be seen in Figure 5. The examination of pore distribution on the vertical plane with regard to the position (height) of the sample was summarised in Fig. 4 and 5. It can be seen that as the height from the bottom is increased (i.e. counter gravity direction), the size and distribution of porosity increased. This is expected since the action of gravity and metallostatic head pressure should be the highest at the bottom of the cast part and thus even if there any porosity, it would be diminished under these effects. It can also be seen that the highest number of pores, total pore area, average

pore area and pore length were achieved by Ti grain refined castings.

When the same alloy was modified with B, these values were dropped. It is interesting to note that as seen in Fig. 3, Ti grain refined melt had the highest bifilm index indicating that the melt quality level lower than B grain refined melt. Thus, these findings lead to the fact that Ti grain refinement causes higher porosity than B grain refinement which is in accordance with the bifilm index results.

The macro images of the horizontal sections of castings are given in Figure 6. In this figure, U1-U4 stands for the position of the sample, 1 being the top and 4 being the bottom.

| Al-10Ti-1B – U1 before degassing | Al-10Ti-1B – U1 after degassing | Al-3B– U1 before degassing | Al-3B– U1 after degassing |
| Al-10Ti-1B – U2 before degassing | Al-10Ti-1B – U2 after degassing | Al-3B– U2 before degassing | Al-3B– U2 after degassing |

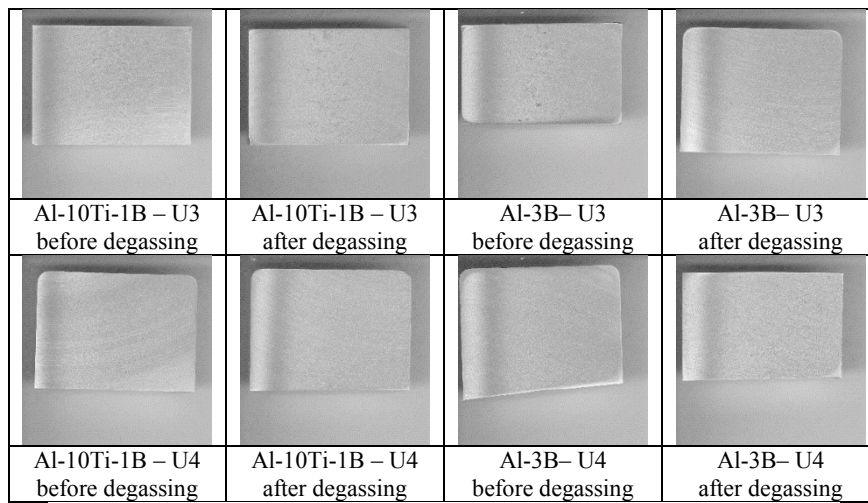| Al-10Ti-1B – U3 before degassing | Al-10Ti-1B – U3 after degassing | Al-3B– U3 before degassing | Al-3B– U3 after degassing |
| Al-10Ti-1B – U4 before degassing | Al-10Ti-1B – U4 after degassing | Al-3B– U4 before degassing | Al-3B– U4 after degassing |

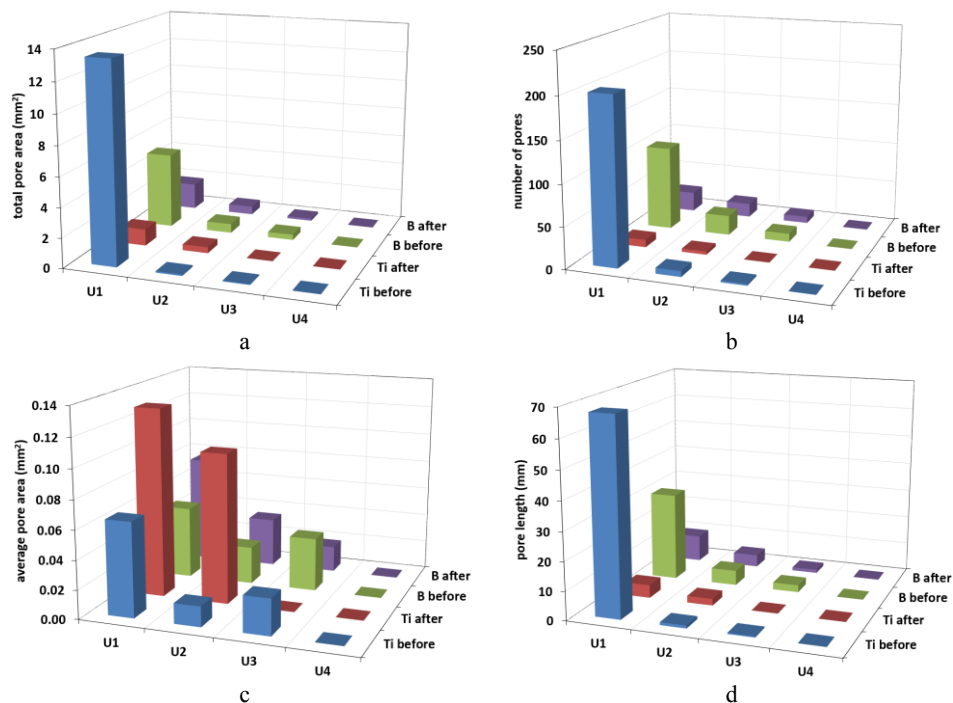Fig. 6. Side view (horizontal) of directionally solidified samples at various heights

Fig. 7. Porosity results of samples taken from the horizontal sections.
a) total pore area, b) number of pores, c) average pore area, d) pore length (Before and after donates to "degassing")

Image analysis results of Figure 6 was summarised as pore size, number, area and distribution in Figure 7.

The size and distribution of pores along the Z axis (horizontal examination) is far more linear than the X-Y axis (vertical examination) results. In Fig. 4 and 5, there is not much clear relationship between the height (U - position) of the sample and the pore parameters. However, in Fig. 6 and 7, the trend appears to be near-to-linear. The pore parameters are decreasing as the height is changed from top to the bottom of the cast part. This is true for both of the melts: Ti grain refined and B-grain refined castings.

This suggested that the pores that are forming along the solidification path (i.e. reserve direction to the heat flow), are more homogeneous. The absence of pores on the sides of the cast part is understandable since solidification starts from the mould wall and due to rapid cooling, pore formation is hindered. On the other hand, pores in the centre of the cylindrical bars raises a question because there should be liquid head that should feed the solidified cast part in the centre. However, the size, shape and distribution of pores that are along the solidification path in centre have heterogeneous and unpredicted size and shapes. This phenomenon can be explained easily by the presence of bifilms.

Higher the population of bifilms (i.e. high bifilm index) increases chance of feeding problems. Therefore, it is important to note that the most significant correlation between location and density of pores was achieved with bifilm index measurements.

4. Conclusions

There is a good correlation between bifilm index and porosity formation in the directionally solidified A356 alloy. As the bifilm index increases, the number, size and area of porosity increases.

With the degassing of the melt, bifilm index was decreased because bifilms were removed from the melt and thus porosity was decreased.

Ti-free B grain refinement leads to lowered porosity and better feeding in Al-Si alloys.

References

[1] Campbell, J. (2003). *Castings: [the new metallurgy of cast metals]*. Butterworth Heinemann.

[2] Zimmermann, G., Sturz, L., Walterfang, M. & Dagner, J. (2009). Effect of melt flow on dendritic growth in AlSi7-based alloys during directional solidification. *International Journal of Cast Metals Research*. 22(1-4). 10.1179/136404609X368154.

[3] Dold, P. & Benz, K.W. (1999). Rotating magnetic fields: Fluid flow and crystal growth applications. *Progress in Crystal Growth and Characterization of Materials*. 38(1).

[4] Goto, I., Horiuchi, S. & Anzai, K. (2011). Defect formation mechanism in directional solidification method using chills and high temperature mould. *International Journal of Cast Metals Research*. 24(3-4). 10.1179/136404611 X13001922708795.

[5] Arnberg, L. & Mathiesen, R.H. (2007). The real-time, high-resolution x-ray video microscopy of solidification in aluminum alloys. *Jom*. 59(8).

[6] Dong, H. & Lee, P. (2005). Simulation of the columnar-to-equiaxed transition in directionally solidified Al–Cu alloys. *Acta Materialia*. 53(3).

[7] Kurz, W. & Fisher, D.J. (1981). Dendrite growth at the limit of stability: tip radius and spacing. *Acta Metallurgica*. 29(1).

[8] McCartney, D. (1989). Grain refining of aluminium and its alloys using inoculants. *International Materials Reviews*. 34(1).

[9] Reinhart, G., Mangelinck-Noël, N., Nguyen-Thi, H., Schenk, T., Gastaldi, J., Billia, B., Pino, P., Härtwig, J. & Baruchel, J. (2005). Investigation of columnar–equiaxed transition and equiaxed growth of aluminium based alloys by X-ray radiography. *Materials Science and Engineering: A*. 413.

[10] Kori, S.A., Murty, B.S. & Chakraborty, M. (2000). Development of an efficient grain refiner for Al-7Si alloy and its modification with strontium. *Materials Science and Engineering: A*. 283(1-2), 94-104.

[11] Sigworth, G. & Guzowski, M. (1985). Grain refinement of hypoeutectic Al-Si alloy [J]. *AFS Transaction*. 93.

[12] Wang, X. (2005). The formation of AlB2 in an Al-B master alloy [J]. *Journal of Alloys and Compounds*. 403.

[13] Dispinar, D. & Campbell, J. (2006). Use of bifilm index as an assessment of liquid metal quality. *International Journal of Cast Metals Research*. 19(1).

[14] Dispinar, D. & Campbell, J. (2004). Critical assessment of reduced pressure test. Part 2: Quantification. *International Journal of Cast Metals Research*. 17(5).

[15] Dispinar, D. & Campbell, J. (2013). Reduced Pressure Test (RPT) For Bifilm Assessment. in *Shape Casting: 5th International Symposium 2014*. (Page Range). John Wiley & Sons, Inc.